Table 2S U-Pb age of HJLG241 monazite using LA-SF-ICP-MS including analytical method and individual U-Pb data from the same place HJLG241 beryl

In situ U–Pb dating of monazite grains from the HJLG sample, co-located with beryl HJLG241, was carried out using laser ablation–sector field–inductively coupled plasma–mass spectrometry (LA–SF–ICP–MS). Analyses were performed with a Thermo Fisher Scientific Element XR HR–ICP–MS instrument coupled to a 193 nm ArF excimer laser system (Geolas HD, Lambda Physik, Göttingen, Germany) at the State Key Laboratory of Lithospheric Evolution, Institute of Geology and Geophysics, Chinese Academy of Sciences (IGGCAS), Beijing.

Prior to routine analyses, the instrument was tuned using a standard solution to optimize sensitivity and mass stability, and the detector P/A (pulse/analog) factor was corrected to ensure linear response between pulse and analog modes. During laser ablation, helium was used as the carrier gas and mixed with argon before entering the ICP torch. The laser parameters were set to a spot diameter of 10 µm, an energy density of 4.0 J·cm^{-2}, and a repetition rate of 2 Hz.

The monazite standard RW-1 (recommended $^{207}Pb/^{235}U$ age = 904.15 ± 0.26 Ma; Ling et al., 2017) was used as the primary reference standard. Diamantina ($^{207}Pb/^{235}U$ age = 495.26 ± 0.54 Ma; Gonçalves et al., 2018) and Bananeira ($^{207}Pb/^{235}U$ age = 507.7 ± 1.3 Ma; Gonçalves et al., 2016) monazites were analyzed as secondary standards to monitor reproducibility and accuracy. NIST SRM 612 and ARM-1 glasses were used as reference materials for trace element quantification (Wu et al., 2019; Wu et al., 2021).

The following isotopes were monitored during analysis: ^{202}Hg, $^{204}(Hg + Pb)$, ^{206}Pb, ^{207}Pb, ^{208}Pb, ^{232}Th, ^{235}U, and ^{238}U. Dwell times for each mass are listed in Table S2-1. The $^{207}Pb/^{235}U$ ratio was calculated using the measured ^{238}U signal and assuming a $^{238}U/^{235}U$ ratio of 137.818. Data reduction, including instrumental mass bias correction and calibration of isotopic fractionation for $^{207}Pb/^{206}Pb$, $^{206}Pb/^{238}U$, $^{207}Pb/^{235}U$, and $^{208}Pb/^{232}Th$ ratios, was performed using Iolite 4.0 software.

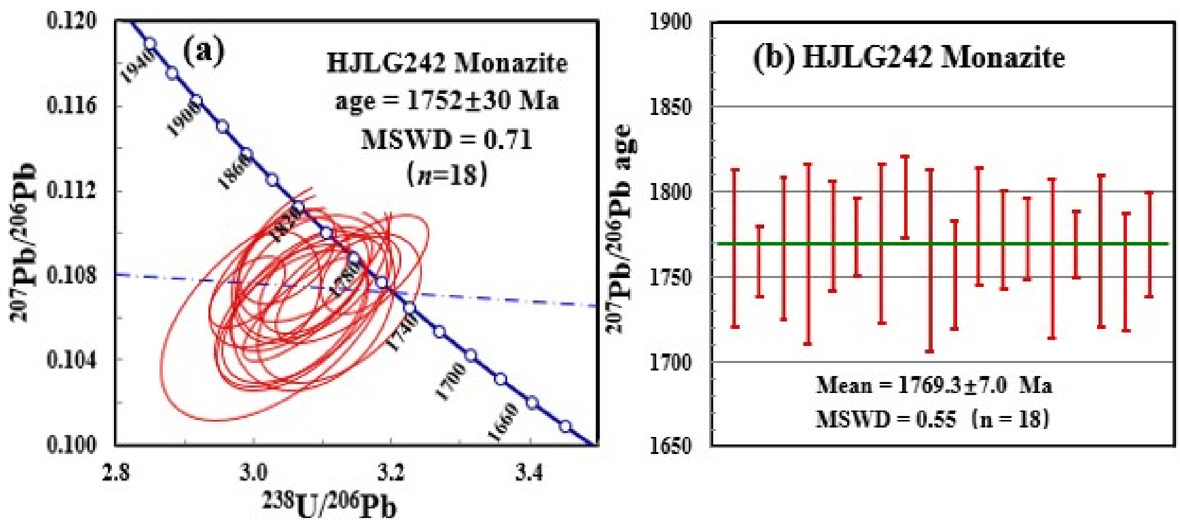

Figure S1. Monazite U-Pb Tera-Wasserburg diagram of sample HJLG242 in this study. (a) Monazite U-Pb Tera-Wasserburg diagram of sample HJLG242, (b) Monazite Pb-Pb age of sample HJLG242, MSWD = mean square of weighted deviates. Data were plotted and evaluated using Isoplot (Ludwig, 2003). Error bars in the insets are at the 2s level.

Each analytical spot consisted of approximately 5 s of background measurement followed by 40 s of ablation. The weighted mean $^{207}Pb/^{206}Pb$ age and U–Pb concordia age were calculated using Isoplot (Ludwig, 2003). As shown in Figure S1, the monazite sample HJLG242 yields a weighted mean $^{207}Pb/^{206}Pb$ age of 1769.3 ± 7.0 Ma (2σ, n = 18), agree well with its U–Pb Tera–Wasserburg age of 1752 ± 30 Ma (2σ, n = 18). These results are in good agreement with the Rb–Sr age of beryl HJLG241 (1788 ± 35 Ma, 2σ, n = 20), confirming the reliability of the Rb–Sr dating results. The detailed analytical conditions are provided in Table S2-1, and the individual U–Pb isotopic data for HJLG242 are listed in Table S2-2.

References

1. X. X. Ling, M. H. Huyskens, Q. L. Li, Q. Z. Yin, R. Werner, Y. Liu, G. Q. Tang, Y. N. Yang and X. H. Li, Miner. Petrol.,

2017, 111, 163–172.
2. G. O. Gonçalves, C. Lana, R. Scholz, I. S. Buick, A. Gerdes, S. L. Kamo, F. Corfu, D. Rubatto, M. Wiedenbeck, H. A. Nalini Jr. and L. C. A. Oliveira, Geostand. Geoanal. Res., 2018, 42, 25–47.
3. G. O. Gonçalves, C. Lana, R. Scholz, I. S. Buick, A. Gerdes, S. L. Kamo, F. Corfu, M. M. Marinho, A. O. Chaves, C. Valeriano and H. A. Nalini Jr., Chem. Geol., 2016, 424, 30–50.
4. S. T. Wu, G. Wörner, K. P. Jochum, B. Stoll, K. Simon and A. Kronz, Geostand. Geoanal. Res., 2019, 43, 567–584.
5. S. T. Wu, Y. H. Yang, K. P. Jochum, R. L. Romer, J. Glodny, I. P. Savov, S. Agostini, J. C. De Hoog, S. T. Peters and A. Kronz, Geostand. Geoanal. Res., 2021, 45, 719–745.
6. K. R. Ludwig, Berkeley Geochronol. Cent. Spec. Publ., 2003, 4, 71.
7. S. T. Wu, M. Yang, Y. H. Yang, L. Xie, C. Huang, H. Wang and J. H. Yang, Int. J. Mass Spectrom., 2020, 456, 116394.
8. Z. Liu, F. Wu, Y. Yang, J. H. Yang and S. A. Wilde, Chem. Geol., 2012, 334, 221–239.
9. U. Schärer, Earth Planet. Sci. Lett., 1984, 67, 191–204.

Table 2S-1 Individual instrumental parameters for in situ U-Pb dating.

Laser ablation system	
Make, model, and type	Coherent, GeoLas HD
Ablation cell and volume	In-house cell, volume < 3 cm^3
Laser wavelength	193 nm
Pulse width	~20 ns
Energy density/fluence	~4 J cm^{-2}
Repetition rate	2 Hz
Spot size	10 µm
Sampling mode/pattern	Single-hole drilling
Ablation gas flow (He)	~0.75 L min^{-1}
Ablation duration	40 s
ICP-MS or ICP-MS/MS	
Make, model, and type	Element XR
RF power	1320 W
Guard electrode (Pt)	Connected
Sample cone	Jet sample cone
Skimmer cone	H-version skimmer cone
Coolant gas flow (Ar)	15.0 L min^{-1}
Auxiliary gas flow (Ar)	0.80 L min^{-1}
Carrier gas flow (Ar)	0.95 L min^{-1}
Enhancement gas flow (N_2)	-4 mL min^{-1}
Scan mode	E-scan
Isotopes measured (m/z) and dwell times	^{202}Hg(2ms), ^{204}Pb(2ms), ^{206}Pb(15ms), ^{207}Pb(25ms) , ^{208}Pb(2ms), ^{232}Th(2ms), ^{235}U(10ms), ^{238}U(10ms)
Detection system	Counting and analogue
Resolution (M/ΔM)	~300
Total integration time	0.27 s

Table 2S-2 Individual U-Pb data of HJLG242 by LA-SF-ICP-MS in this study.

Sample	Data for Wetherill plot						Apparent dates (Ma)					
	$^{207}Pb/^{206}Pb$	2s	$^{207}Pb/^{235}U$	2s	$^{206}Pb/^{238}U$	2s	$^{207}Pb/^{206}Pb$	2s	$^{207}Pb/^{235}U$	2s	$^{206}Pb/^{238}U$	2s
HJLG242-1	0.1079	0.0025	4.880	0.133	0.3239	0.0096	1767	46	1796	23	1807	47
HJLG242-2	0.1079	0.0012	4.943	0.066	0.3344	0.0051	1759	20	1808	11	1858	25
HJLG242-3	0.1084	0.0025	4.772	0.133	0.3253	0.0104	1767	42	1778	23	1814	51
HJLG242-4	0.1082	0.0031	4.829	0.198	0.3297	0.0148	1763	53	1786	35	1835	72
HJLG242-5	0.1086	0.0019	4.730	0.095	0.3182	0.0091	1774	33	1768	17	1776	46
HJLG242-6	0.1087	0.0014	4.810	0.096	0.3240	0.0068	1773	23	1784	17	1807	33
HJLG242-7	0.1086	0.0027	4.885	0.121	0.3297	0.0057	1770	47	1798	21	1836	28
HJLG242-8	0.1101	0.0015	4.925	0.092	0.3280	0.0062	1797	24	1804	16	1827	30
HJLG242-9	0.1080	0.0032	4.767	0.183	0.3241	0.0103	1759	53	1776	32	1808	50
HJLG242-10	0.1075	0.0018	4.774	0.130	0.3271	0.0097	1751	31	1777	23	1822	47
HJLG242-11	0.1091	0.0021	4.823	0.103	0.3259	0.0089	1779	34	1787	18	1817	43
HJLG242-12	0.1087	0.0017	4.889	0.124	0.3293	0.0089	1772	29	1796	21	1833	43
HJLG242-13	0.1087	0.0014	4.852	0.146	0.3242	0.0095	1772	24	1791	25	1806	47
HJLG242-14	0.1080	0.0028	4.700	0.140	0.3203	0.0099	1761	46	1765	25	1790	49
HJLG242-15	0.1085	0.0011	4.722	0.075	0.3170	0.0048	1769	19	1768	13	1774	23
HJLG242-16	0.1083	0.0026	4.791	0.132	0.3275	0.0097	1765	44	1788	26	1825	47
HJLG242-17	0.1075	0.0020	4.776	0.069	0.3255	0.0077	1753	34	1780	12	1815	38
HJLG242-18	0.1084	0.0018	4.786	0.119	0.3228	0.0085	1769	31	1776	21	1800	41
average	0.1084		4.786		0.3228		1769		1776		1800	
sd	0.0018		0.119		0.0085		31		21		41	
rsd(%)	1.7%		2.5%		2.6%		1.8%		1.2%		2.3%	